Supplement of The Cryosphere, 20, 551–572, 2026
https://doi.org/10.5194/tc-20-551-2026-supplement

The Cryosphere Open Access EGU

Supplement of

Dynamics of snow and glacier cover in the Upper Karnali Basin, Nepal: an analysis of its relationship with climatic and topographic parameters

Motilal Ghimire et al.

Correspondence to: Motilal Ghimire (motighimire@gmail.com)

Supplementary Material

Sect. S1: Snow-cover data (Landsat)

Snow-cover mapping was generated using Landsat Surface Reflectance images from Landsat 5 TM, Landsat 7 ETM+, and Landsat 8 OLI. For the period preceding the Scan Line Corrector (SLC) failure, only Landsat 7 ETM+ images (2002–2003) were used. For subsequent years, Landsat 5 TM and Landsat 8 OLI images were used. Additionally, Landsat sensors are susceptible to interference from clouds and shadows, particularly during the monsoon season. These factors influenced the selection of scenes and introduce uncertainty into the snow-cover measurements.

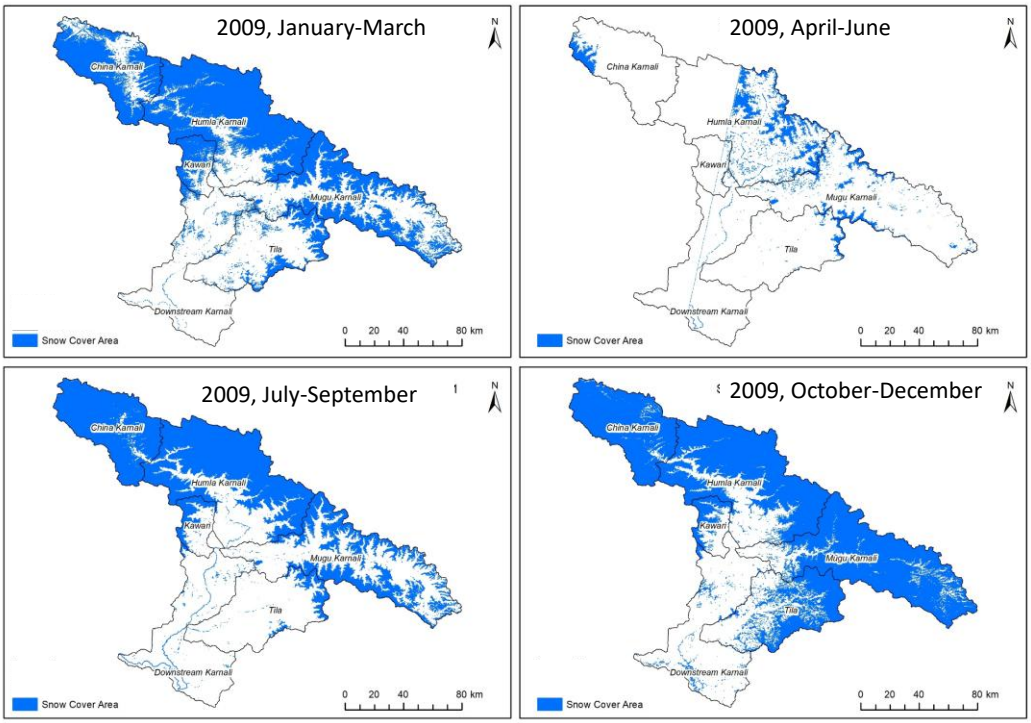

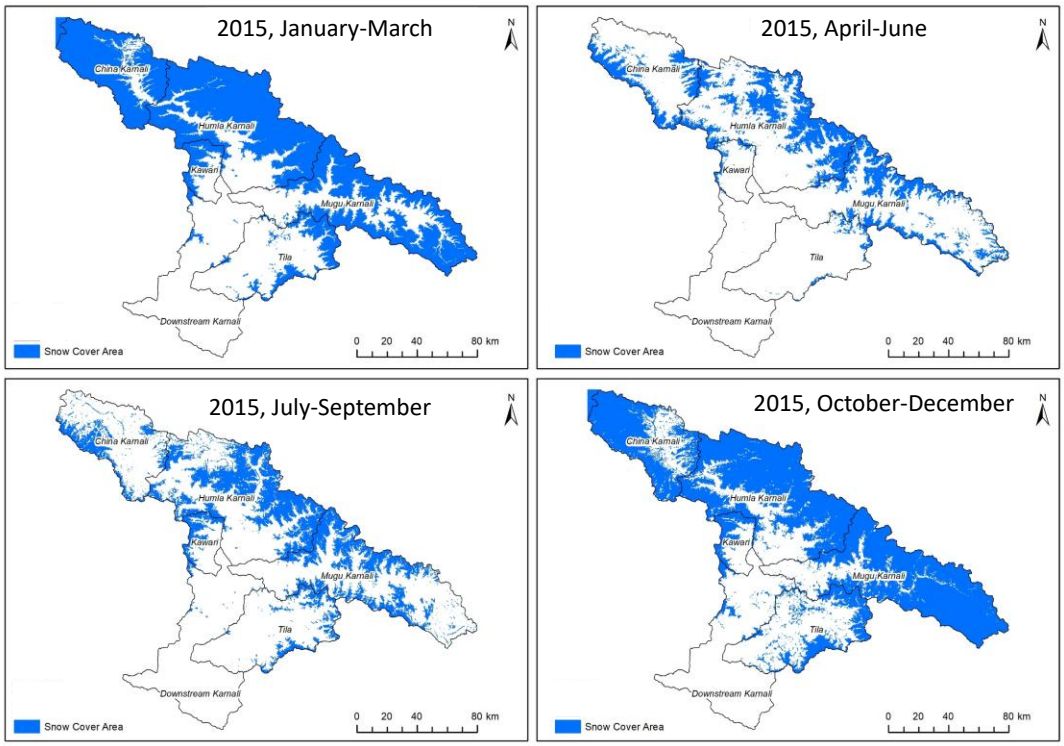
2015, January-March
2015, April-June
2015, July-September
2015, October-December
China Karnali
Humla Karnali
Kawari
Mugu Karnali
Tila
Downstream Karnali
Snow Cover Area
0 20 40 80 km
N

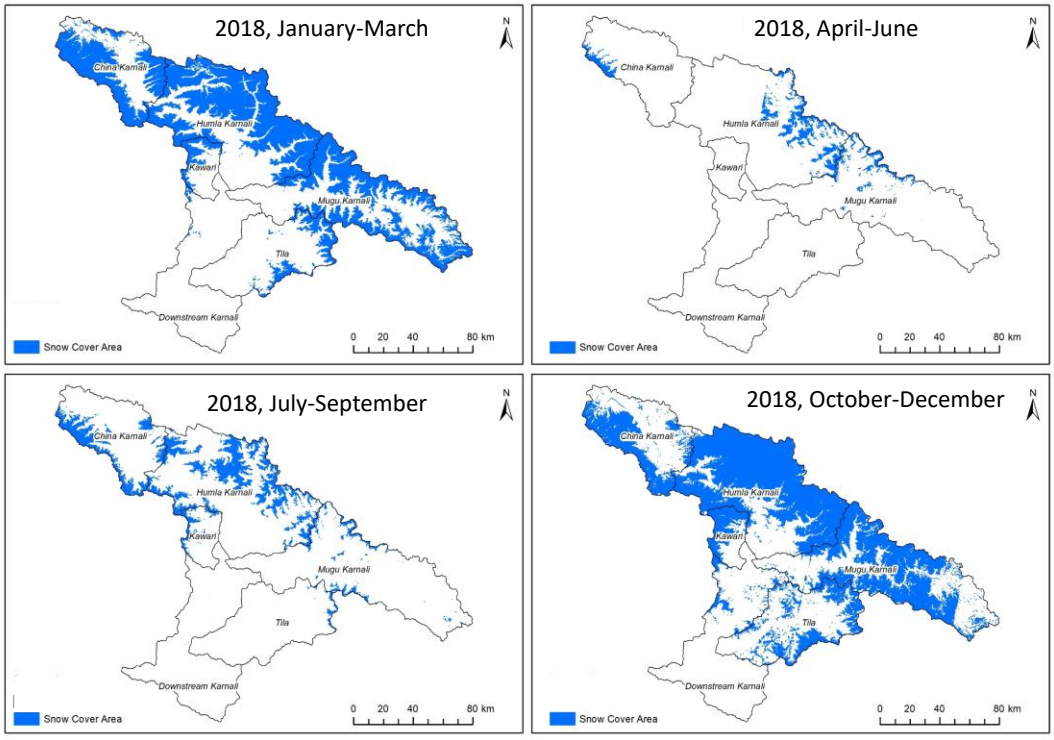
2018, January-March
2018, April-June
2018, July-September
2018, October-December
China Karnali
Humla Karnali
Kawari
Mugu Karnali
Tila
Downstream Karnali
Snow Cover Area
0 20 40 80 km
N

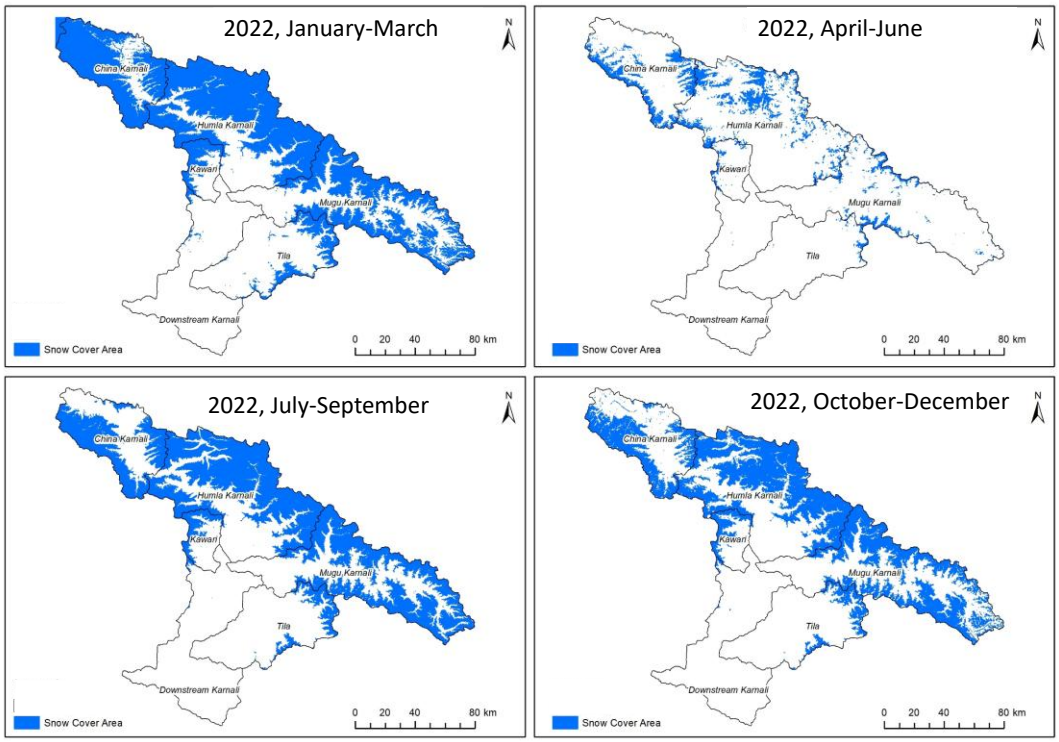

Figure S1. Snow cover data derived from Landsat 7 and 8 for different periods. The data shows the limitations and scope of Landsat 7 and 8 data.

Sect. S2: Validation and accuracy assessment

We evaluated the spatial agreement between Landsat and MODIS snow-cover products using a multi-step validation approach following Rittger et al. (2020). First, we resampled Landsat-derived snow-cover area (SCA) maps from a 30-meter resolution to 500 meters using a majority-aggregation technique to align with the MODIS MOD10A2 grid. This resampling enabled direct pixel-by-pixel comparison while maintaining the dominant snow and non-snow classifications. During snow detection, we applied a Normalized Difference Vegetation Index (NDVI) filter to minimize misclassification between snow and vegetation in mixed or forested areas, consistent with Rittger et al. (2013). This adjustment reduced false snow detections at lower elevations and enhanced consistency with MODIS classifications.

From each resampled Landsat image (covering 185 × 180 km), we randomly selected approximately 10% of the pixels (around 13,000) to represent the categories of snow, non-snow, and cloud. These points were then overlaid onto the corresponding MODIS

MOD10A2 images, and pixel values were extracted to create a composite attribute table for statistical analysis.

We evaluated classification accuracy using confusion matrices for six validation scenes with low cloud cover (<7%), distributed across various topographic and climatic regions. The results showed overall accuracies ranging from 77.5% to 94.9%, with Kappa coefficients between 0.68 and 0.89, consistent with previous MODIS validation studies (Tables S1 and S2; Hall and Riggs, 2007; Painter et al., 2009).

Sub-scene analyses revealed that MODIS systematically overestimated snow cover, with snow-covered areas 1.3 to 1.6 times larger than those derived from Landsat. We attribute this discrepancy to mixed-pixel effects and the coarser spatial resolution of MODIS (Dozier et al., 2008; Gafurov and Bárdossy, 2009) (Table S3). This bias corroborates earlier findings that MODIS tends to overestimate snow extent in heterogeneous mountainous terrain (Rittger et al., 2013; Tang et al., 2017).

Although the MODIS MOD10A2 product provides reliable basin-scale snow cover area (SCA) estimates (Dietz et al., 2012), we interpreted trends–particularly those during the monsoon season–with caution due to residual cloud effects and spatial averaging.

Table S1. Example confusion matrix comparing MODIS MOD10A2 snow classification (500 m) with Landsat snow classification resampled from 30 m to 500 m. Values are counts; accuracies are in percent.

	MODIS Non-snow	MODIS Snow	Total	User's accuracy (%)
Landsat Non-snow	8950	2472	11422	78.35
Landsat Snow	144	4744	4888	97.05
Total	9094	7216	16310	
Producer's accuracy (%)	98.4	65.7		

Overall accuracy = 83.97%.

Table S2. Landsat Surface Reflectance scenes used for validating MODIS MOD10A2 snow classification (500 m), including acquisition date (as in source metadata), cloud cover percentage, overall accuracy (percent), and broad region of Nepal (MW = Mid-West, FW = Far-West, E = East).

Date	Cloud cover %	Overall accuracy (%)	Region of Nepal
2020-03-08	6.52	83.96	MW
2021-03-27	4.45	94.89	MW
2021-03-02	5.2	86.21	FW
2021-12-31	2.36	77.59	FW
2021-04-23	6.9	97.62	E
2019-21-19	5.29	97.22	E

Table S3. Comparison of snow-covered area derived from MODIS MOD10A2 (500 m) and Landsat (30 m) for selected scenes. Exaggeration factor is defined as (MODIS area) / (Landsat area).

Date of scene	Region	Area (ha), MODIS (500 m)	Area (ha), Landsat (30 m)	Exaggeration factor
2020-03-08	MW	571,950	432,200	1.32
2021-03-27	MW	171,425	120,860	1.42
2021-02-03	FW	118,400	73,418	1.61
2021-12-31	FW	301,075	183,355	1.64

References

Bajracharya, S. R., Maharjan, S. B., Shrestha, F., Bajracharya, O. R., and Baidya, S.: Glacier status in Nepal and decadal change from 1980 to 2010 based on Landsat data, International Centre for Integrated Mountain Development (ICIMOD), Kathmandu, Nepal, Research Report 2014/2, 184 pp., ISBN 978-92-9115-311-4, 2014.

Dietz, A. J., Kuenzer, C., Gessner, U., and Dech, S.: Remote sensing of snow – a review of available methods, Int. J. Remote Sens., 33, 4094–4134, https://doi.org/10.1080/01431161.2011.640964, 2012.

Dozier, J., Green, R. O., Nolin, A. W., and Painter, T. H.: Interpretation of snow properties from imaging spectrometry, Remote Sens. Environ., 113, S25–S37, https://doi.org/10.1016/j.rse.2007.07.029, 2008.

Gafurov, A. and Bárdossy, A.: Cloud removal methodology from MODIS snow cover product, Hydrol. Earth Syst. Sci., 13, 1361–1373, https://doi.org/10.5194/hess-13-1361-2009, 2009.

Gorelick, N., Hancher, M., Dixon, M., Ilyushchenko, S., Thau, D., and Moore, R.: Google Earth Engine: Planetary-scale geospatial analysis for everyone, Remote Sens. Environ., 202, 18–27, https://doi.org/10.1016/j.rse.2017.06.031, 2017.

Hall, D. K. and Riggs, G. A.: Accuracy assessment of the MODIS snow products, Hydrol. Process., 21, 1534–1547, https://doi.org/10.1002/hyp.6715, 2007.

Hall, D. K., Riggs, G. A., and Salomonson, V. V.: MODIS/Terra Snow Cover 5-Min L2 Swath 500 m, Version 5, NASA National Snow and Ice Data Center Distributed Active Archive Center, Boulder, Colorado, 2006.

Maskey, S., Uhlenbrook, S., and Ojha, S.: An analysis of snow cover changes in the Himalayan region using MODIS snow products and in-situ temperature data, Clim. Change, 108, 391–400, https://doi.org/10.1007/s10584-011-0181-y, 2011.

Painter, T. H., Rittger, K., McKenzie, C., Slaughter, P., Davis, R. E., and Dozier, J.: Retrieval of subpixel snow-covered area and grain size from imaging spectrometer data, Remote Sens. Environ., 113, 1964–1976, https://doi.org/10.1016/j.rse.2009.01.001, 2009.

Parajka, J. and Blöschl, G.: The value of MODIS snow cover data in validating and calibrating conceptual hydrologic models, J. Hydrol., 358, 240–258, https://doi.org/10.1016/j.jhydrol.2008.06.006, 2008.

Rittger, K., Painter, T. H., and Dozier, J.: Assessment of methods for mapping snow cover from MODIS, Adv. Water Resour., 51, 367–380, https://doi.org/10.1016/j.advwatres.2012.03.002, 2013.

Rittger, K., Raleigh, M. S., Dozier, J., Hill, A. F., Lutz, J. A., and Painter, T. H.: Canopy adjustment and improved cloud detection for remotely sensed snow cover mapping, Water Resour. Res., 55, e2019WR024914, https://doi.org/10.1029/2019WR024914, 2020.

Tang, Z., Wang, X., Wang, J., Wang, X., Li, H., and Jiang, Z.: Spatiotemporal variation of snow cover in Tianshan Mountains, Central Asia, based on cloud-free MODIS fractional snow cover product, 2001–2015, Remote Sens., 9, 1045, https://doi.org/10.3390/rs9101045, 2017.

Wan, Z., Hook, S., and Hulley, G.: MOD11A2 MODIS/Terra Land Surface Temperature/Emissivity 8-Day L3 Global 1 km SIN Grid V006, NASA EOSDIS Land Processes Distributed Active Archive Center (LP DAAC), https://doi.org/10.5067/MODIS/MOD11A2.006, 2015.